

Computation of the Plume of an Anode-Layer Hall Thruster

Iain D. Boyd*

Cornell University, Ithaca, New York 14853

A numerical model is presented for simulating the plume of the D55 anode-layer Hall thruster. A combination of the particle-in-cell method for the plasma dynamics and the direct simulation Monte Carlo method for collisions is employed. Ions and neutral atoms are treated as particles, and electrons are assumed isothermal and governed by the Boltzmann relation. A conservative particle weighting scheme is employed to allow accurate resolution of the ions. Assessment of the models employed is made through comparison of the numerical results with experimental measurements taken in two different facilities. The data comparisons are conducted in both the near and far fields of the plume and consist of macroscopic properties such as the plasma potential and microscopic characteristics such as the ion energy distribution function. The agreement obtained between simulation and measurements is in general quite good for all properties considered. Further numerical and experimental work is required to improve the modeling in the far field and off-axis regions of the Hall thruster plume.

Introduction

ACCURATE simulation of plumes from electric propulsion devices is required for assessment of spacecraft integration effects. For engines such as Hall thrusters and ion thrusters that produce plume flows with a large degree of ionization, the main concern is deposition of heavy metallic ions on sensitive spacecraft surfaces. These ions originate in sputtering processes involving high-energy ions inside the engines. The metallic ions may be accelerated into the backflow region behind these thrusters because of the formation of a charge-exchange plasma. An additional concern for Hall thrusters, which have relatively large plume-spreading angles, is direct impingement of the energetic plume on spacecraft surfaces. This may cause heating of sensitive surfaces, or sputtering, leading to secondary contamination effects.

The plumes of xenon ion and Hall thrusters have been modeled in several studies using similar particle methods. Computations of ion-thruster plumes were performed by Samanta Roy et al.,¹ VanGilder et al.,² and Katz et al.³ In Ref. 1 the particle-in-cell (PIC) method⁴ was employed to accelerate ions in self-consistent electrostatic fields. The Boltzmann relation was employed to model the behavior of the electrons. Neutral atoms were not included directly in the simulations, and instead a simple source of charge-exchange plasma was employed. The work in Ref. 2 went beyond this approach by employing the direct simulation Monte Carlo (DSMC)⁵ method to compute the properties of the neutral atoms and to simulate directly the charge-exchange collisions. The PIC method was again employed to accelerate the ions. In Ref. 3 a modification to the Boltzmann relation was proposed to account for trapping of source electrons.

Hybrid particle-fluid models of the interior flows of Hall thrusters have been presented by Fife et al.⁶ and by Boeuf and Garrigues.⁷ These techniques are not well-suited to plume computations because they do not accurately resolve charge-exchange phenomena, which are an important aspect of the formation of the far-field plume structure.

A combination of the PIC and DSMC methods has been employed by Oh and Hastings⁸ to simulate the plume of the SPT-100 Hall thruster. As with the earlier ion-thruster simulations, a major simplification in Ref. 8 was the use of a constant electron temperature in the Boltzmann relation. Together with an assumption of charge neutrality, this allowed the calculation of the electric potential from the ion density. There is clear experimental evidence that

the electron temperature is not constant in the SPT-100 plume⁹ nor in the D55 (a so-called anode-layer thruster).¹⁰ Of even more concern is the fact that detailed experimental investigation¹¹ has shown that electrons in an SPT-50 plume do not have a Boltzmann energy distribution. Because the properties of the electrons are so important in characterizing the potentials produced in the plasma plume flows and these potentials generate the electric fields that are responsible for determining the fluxes of harmful ions onto the spacecraft surfaces, a more detailed computational approach may be required for simulation of the electrons.

There are two primary goals of the present study. The first goal is to apply a PIC-DSMC scheme similar to that proposed in Ref. 8 to the plume flow from the D55 device. No prior modeling of an anode-layer Hall thruster plume has been reported in the literature. The second goal is to make a critical assessment of the usefulness of the PIC-DSMC procedure for modeling a Hall thruster plume, which is achieved by comparing the model predictions to several different sets of measurements taken in the near and far fields of the D55 plume. The paper first describes the PIC-DSMC computer code and the flow conditions studied. General features of the numerical results are discussed. Comparison is then made of the computational results to several sets of experimental data taken in the plume of the D55. The results are discussed in the context of assessing the accuracy of the model.

Numerical Methods

A PIC-DSMC code is developed that simplifies the plasma dynamics in a manner similar to that described in Ref. 8. The flow domain is axially symmetric. In the usual PIC manner ion positions are used to determine charge density at the nodes of the computational grid. The electrons are assumed to be isothermal and are not included directly in the computation. Instead, the electron number density is obtained from the Boltzmann relation

$$n_e = n_{\text{ref}} \exp(e\phi/kT_e) \quad (1)$$

where n_{ref} is a reference number density, e is the charge of an electron, ϕ is the plasma potential, k is the Boltzmann constant, and T_e is the (constant) electron temperature. Use of the Boltzmann relation assumes that in addition to being collisionless, the electrons are also unmagnetized. Close to the thruster, the electrons will likely be magnetized to some extent. Recall that it is the primary goal of this paper to assess the usefulness of the simple approach of Eq. (1) for modeling the electron behavior through detailed comparisons with experimental measurements.

Unlike Ref. 8, charge neutrality is not assumed in the present work. Instead, the difference between the ion charge density and the electron number density at the grid nodes is used in the Poisson equation to solve for the plasma potential using a standard

Received 28 August 1998; revision received 19 July 1999; accepted for publication 20 July 1999. Copyright © 1999 by the American Institute of Aeronautics and Astronautics, Inc. All rights reserved.

*Associate Professor, Mechanical and Aerospace Engineering; currently Associate Professor, University of Michigan, Ann Arbor, MI 48109; iainboyd@umich.edu. Senior Member AIAA.

alternating-direction-implicit scheme. This approach was previously employed by Roy et al.¹ to compute the plume of an ion thruster. It is again used here not so much because charge neutrality is an issue, but rather to provide a smooth variation in the plasma potential. If the potential is computed at each time step based on the instantaneous number of ion particles, as performed in Ref. 8, there will be significant statistical fluctuation in the potential field because of the finite number of particles employed in the simulation.

The DSMC portion of the code simulates the following types of collisions: Xe-Xe, Xe-Xe⁺, and Xe-Xe⁺⁺. The Xe-Xe collisions employ the variable hard sphere model of Bird.⁵ For neutral-ion collisions both momentum transfer and charge-exchange mechanisms are considered. The Xe-Xe⁺ momentum cross section in units of m² is obtained from the model of Dalgarno et al.¹²:

$$\sigma = 6.416 \times 10^{-16} / g \quad (2)$$

where g is the relative collision velocity. The same form was employed by Oh and Hastings⁸ except that the leading constant was 8.281×10^{-16} and this appears to be a numerical error. The Xe-Xe⁺ charge-exchange cross section in units of m² is obtained from the data fit of Sakabe and Izawa¹³:

$$\sigma = [1.81 \times 10^{-18} - 2.12 \times 10^{-19} \log_{10}(100 * g)] \times (I_o/I)^{-1.5} \quad (3)$$

where I_o is the ionization potential of hydrogen and I is the ionization potential of Xe⁺. Equation (3) gives a better fit to available experimental data in comparison to the theoretical model that formed the basis of the cross section used in Ref. 8. Equation (3) is also used to determine the charge exchange cross section for Xe-Xe⁺⁺ interactions in which I is set to the ionization potential for Xe⁺⁺.

Another difference from the implementation of Ref. 8 in the present work is in the DSMC treatment of trace species. As will be discussed later, when performing simulations of the behavior of the D55 in ground-based vacuum chambers the residual density of neutral xenon atoms is orders of magnitude larger than the densities in the far-field plume of the particles exhausting from the thruster. Numerical weights must be employed in the DSMC code to avoid having to use a very large number of particles in the computation to simulate the residual atoms. In Ref. 8 a weighting scheme from Bird⁵ is employed, despite the fact that Bird recommends against use of this technique. The problem with Bird's scheme is that it conserves momentum and energy only over a large number of collisions. For computing charge-exchange collisions in a Hall thruster plume, there are very few collisions, and the use of a nonconservative weighting scheme may be inappropriate. In the present work a conservative weighting scheme first proposed by Boyd¹⁴ and further developed for charge-exchange collisions by VanGilder and Boyd¹⁵ is employed.

The computation begins with the physical domain initialized to the properties of the ambient medium. For simulation of experiments performed in ground-based facilities, this medium is assumed to consist of neutral xenon at a fixed pressure and temperature. The properties of the medium are maintained by introducing neutral atoms across the computational boundaries with properties consistent with the prescribed pressure and temperature. For simulation of the plume exhausting into space, the medium is simply a vacuum. Particles are introduced into the flowfield at the thruster exit plane using macroscopic values of species number densities, velocities, and temperatures that are consistent with measured device properties. The procedure employed for establishing these macroscopic values is described later. The computational domain extends to 1 m downstream from the thruster exit plane, to 0.6 m radially, and a small portion of the back flow region is also included.

The length scales characterizing the plasma and collision phenomena are the Debye length and the mean free path, respectively. For the conditions at the exit plane typical of Hall thrusters, the Debye length is on the order of 10^{-5} m, whereas the mean free path is on the order of 0.1 m. Thus, in the generation of a computational grid, it is the issue of resolution of the plasma phenomena that dominates. With such a small Debye length, it is reasonable to assume that the plume will be charge neutral (at least for the region under

consideration). Therefore, it is not necessary to resolve the flow at the level of the Debye length. This is fortunate because otherwise the problem would almost be computationally intractable. The computational grid employed in these studies consists of rectangular cells. The smallest cells are those close to the thruster exit and have a length of 5 mm. The largest cells are located close to the edges of the domain and have a maximum size of 2 cm. The timescales of the flow are also determined by the plasma phenomena, and the inverse of the plasma frequency is used. The computations presented in this study typically employed 300,000 particles.

Along the outer edges of the flow domain, the conditions for the PIC component of the simulation are to assume zero electric field normal to the boundary. For the DSMC component any particles crossing these boundaries are removed from the simulation. At the thruster exit surface the electric fields are zero, and charge neutrality is assumed. The simulation is found to recover the flow rate and thrust assumed in determining the flow conditions.

Flow Conditions

A schematic diagram of the D55 device is shown in Fig. 1. The annular anode chamber has a diameter of 55 mm. For the plume simulations the thruster surface is assumed to be isothermal at a temperature of 300 K and to be electronically grounded. In all computations the flow through the cathode is neglected. This flow is three-dimensional and difficult to include in an axially symmetric simulation. In any case, at a typical operating condition¹⁶ the flow rate through the cathode is only 16% of that through the anode.

Two conditions are considered corresponding to two different experimental investigations. Most of the results presented are for a series of experiments conducted at the University of Michigan.¹⁶⁻¹⁸ The D55 thruster was operated at a flow rate of 4.76 mg/s of xenon, a discharge voltage of 300 V, and a current of 4.5 A. The specific impulse under these conditions was previously measured to be 1,810 s (Ref. 19). The fraction of double xenon ions is assumed to be 0.25. At the thruster exit the temperature of the electrons in the Boltzmann relation is taken to be 3 eV, the temperature of the ions is assumed to be 4 eV, and that of the neutrals is assumed to be 750 K. With these parameters a value for the propellant utilization efficiency of 0.89 is required to obtain consistency with the measured thrust and current. A listing of the flow properties assumed at the thruster exit is given in Table 1. One further consideration is the possibility that the flow spreads at the thruster exit. The D55 has a small nozzle-like geometry at the exit, and so plume spreading is expected. In the present work a half angle of 15 deg is assumed, and the radial velocity varies linearly across each half of the exit plane. The backpressure

Table 1 Flow properties assumed at thruster exit plane

Experiment	Species	n, m^{-3}	T, K	$U, \text{m/s}$
Michigan	Xe	3.4×10^{18}	750	281
	Xe ⁺	3.1×10^{17}	46,400	17,750
	Xe ⁺⁺	1.0×10^{17}	46,400	25,100
NASA	Xe	3.7×10^{18}	750	281
	Xe ⁺	2.5×10^{17}	46,400	17,750
	Xe ⁺⁺	1.5×10^{17}	46,400	25,100

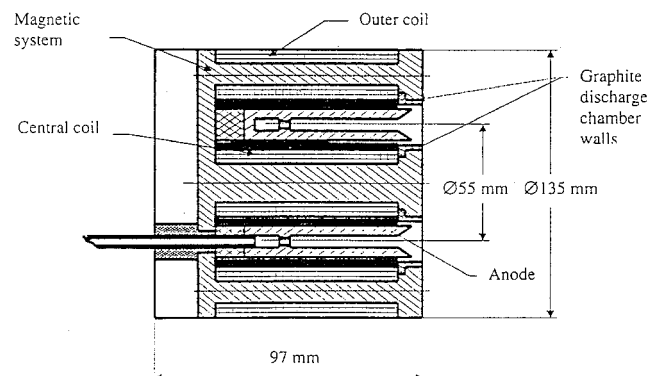


Fig. 1 Schematic diagram of the D55 anode-layer Hall thruster.

in the Michigan facility is reported as 8.3×10^{-3} Pa. Assuming a background temperature of 300 K gives a residual number density of $2 \times 10^{18} \text{ m}^{-3}$. This value is higher than all of the species number densities at the exit of the thruster. Certainly, the number density of background atoms will dominate the thruster species by orders of magnitude far from the thruster. This is the reason that numerical weights are required in the PIC-DSMC simulations to resolve the background particles without requiring an enormous number of particles.

The second flow condition investigated corresponds to a study performed at NASA Lewis Research Center.²⁰ The thruster was operated at a flow rate of 4.52 mg/s and a current of 4.2 A. The backpressure in the NASA chamber was 2.7×10^{-3} Pa. The propellant utilization efficiency consistent with these conditions is calculated to be 0.87. The thruster exit flow conditions for the NASA experiment are also listed in Table 1.

Results

Recall that the primary goal of this investigation is to assess the simple plasma model for computing Hall thruster plumes. This is achieved first through general discussion of the results generated by the PIC-DSMC simulation. Then, the computational results are compared with experimental measurements. In all simulations the reference number density employed in the Boltzmann relation is $1.5 \times 10^{17} \text{ m}^{-3}$. This value is obtained as an average by fitting experimental measurements of electron number density, temperature, and potential reported in Ref. 16 to the Boltzmann relation. Recall that the electron temperature in the Boltzmann relation is assumed constant at 3 eV.

General Features of Simulation Results

First, the effect of facility backpressure is assessed using the simulations. In Fig. 2a contours of plasma potential are shown for the Michigan facility and for vacuum expansion. In both simulations the thruster exit plane properties are those for the Michigan experi-

ment. Although the two sets of results are in agreement close to the thruster, it is clear that the finite backpressure in the Michigan chamber has significantly affected the off-axis and backflow regions. By consideration of the gradients in potential, it is clear that significant electric fields are generated in the plume. The lobe structures seen directly above the thruster exit in the vacuum simulation are produced by the charge-exchange plasma. In Fig. 2b contours of the number density of Xe^+ are shown for the Michigan and vacuum conditions. Again it is clear that the vacuum chamber has inhibited the expansion of the plume into the off-axis and back flow regions.

Flow properties of the three species for plume expansion into vacuum are compared along the plume axis in Figs. 3a–3c. The number density profiles shown in Fig. 3a indicate that both neutral and charged species densities decay at about the same rate beyond a

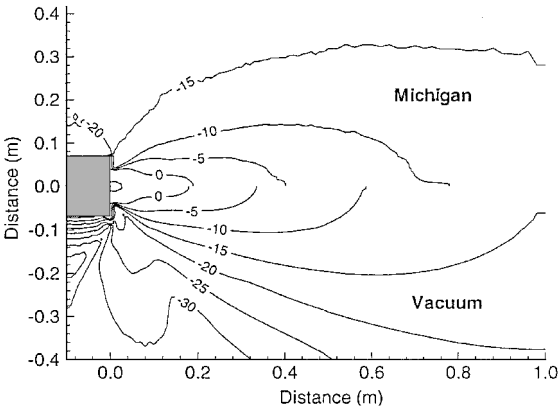


Fig. 2a Contours of plasma potential in volts.

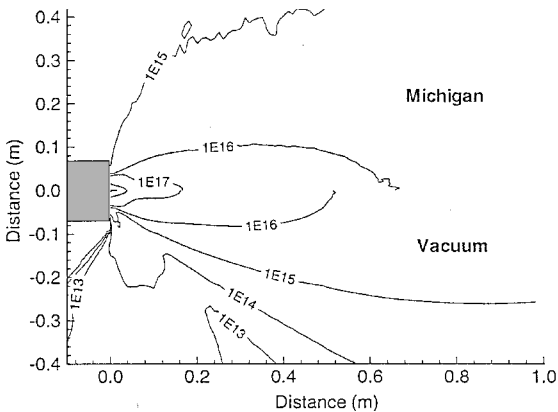


Fig. 2b Contours of Xe^+ number density in m^{-3} .

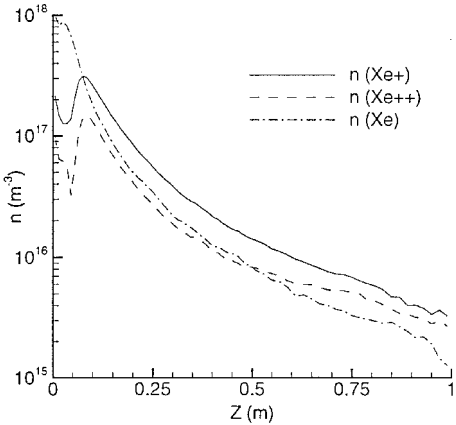


Fig. 3a Number density along the plume axis.

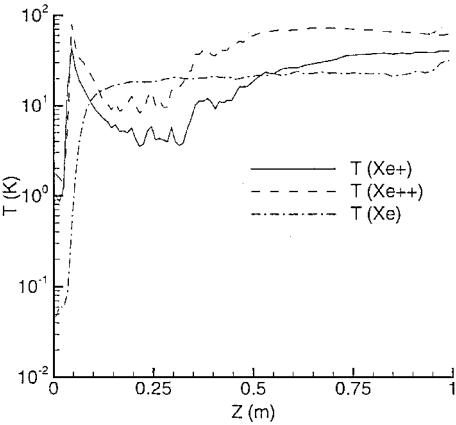


Fig. 3b Temperature along the plume axis.

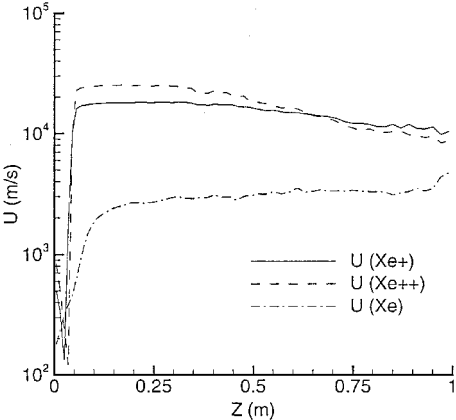


Fig. 3c Velocity along the plume axis.

distance of about 10 cm from the thruster exit plane. This is mainly caused by charge-exchange phenomena. This is more clearly illustrated in Fig. 3b, which shows the temperature profiles of the three species. Consider first the behavior of the ions. In general, the profiles of Xe^+ and Xe^{++} follow one another. At the exit plane the temperatures are a few eV, and they quickly rise to peak values of 30–50 eV. These values have to be interpreted with care. In particle methods the temperature is essentially computed as the variance of the velocity distribution function. In a plasma with a significant degree of charge exchange, the velocity distribution functions are very wide. There is a population of ions at large velocities (about 18,000 m/s) that originated from the thruster and a population of

low velocity (about 1,000 m/s) charge-exchange ions. The temperature for the Xe^{++} ions is larger than that for Xe^+ because the high-velocity population is centered around 25,000 m/s. The atom temperature grows to a value similar to that for Xe^+ caused by charge-exchange collisions. Far from the thruster the velocity distribution of atoms will closely resemble that for the single-charged ions. Comparison of the velocities shown in Fig. 3c again illustrates the similarity in behavior of the ions and the effect of charge exchange on the atoms.

The same comparisons are made along a radial line located 50 cm from the thruster in Figs. 4a–4c. Figure 4a shows the differences in the gas dynamic and plasma acceleration mechanisms. There is generally a strong negative gradient in plasma potential in the radial direction, and this leads to acceleration of the ions. Hence, the rate of decay of the ion densities is greater than that for the neutral atoms. The temperature profiles shown in Fig. 4b indicate that the increase in neutral atom temperature caused by charge exchange is at a maximum on the axis. Far from the axis the neutral temperature is orders of magnitude lower than the ion temperatures. Recall again that these temperatures are more a measure of the spread of the velocity distribution function than a measure of the total internal energy. The velocity profiles shown in Fig. 4c again indicate that at large distances from the axis the neutral atoms are unaffected by charge exchange.

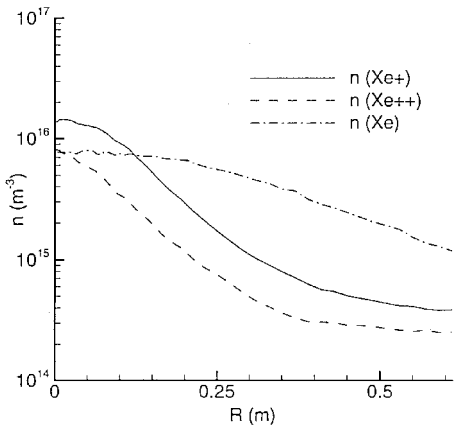


Fig. 4a Number density along the radial line at 0.50 m from the thruster exit.

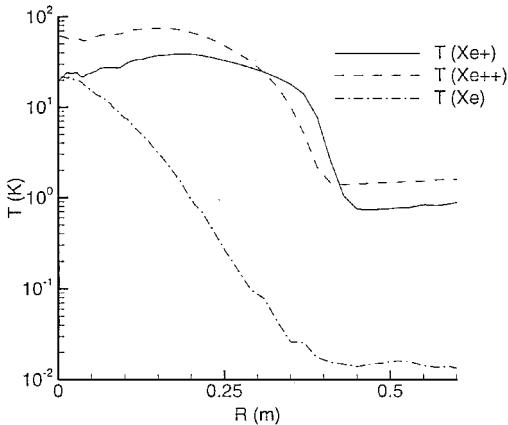


Fig. 4b Temperature along the radial line at 0.50 m from the thruster exit.

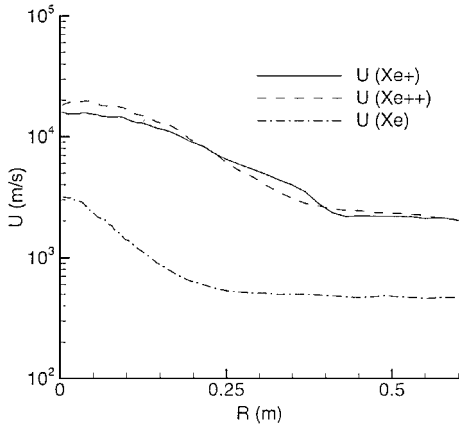


Fig. 4c Velocity along the radial line at 0.50 m from the thruster exit.

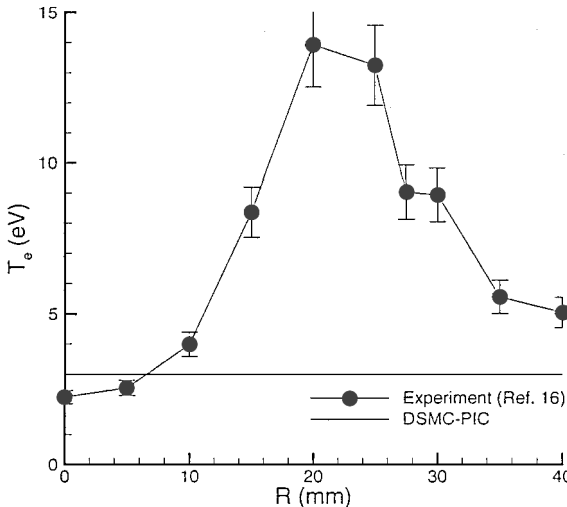


Fig. 5a Radial profile of electron temperature at 10 mm from the thruster exit plane.

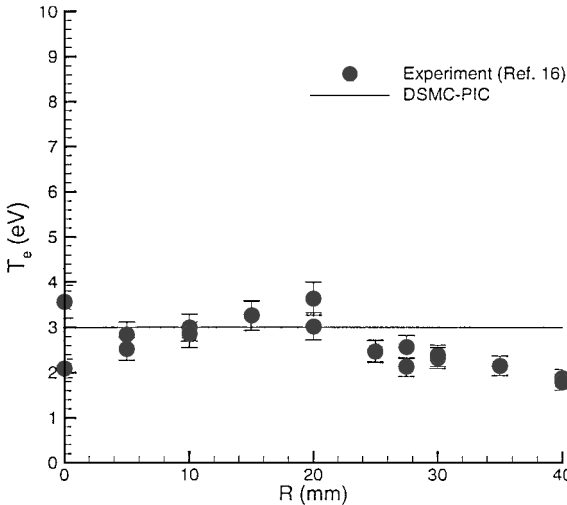


Fig. 5b Radial profile of electron temperature at 50 mm from the thruster exit plane.

Comparison with Experimental Data

A series of probe experiments were conducted by Domonkos et al.¹⁶ in the near field of the D55 plume. Faraday probes were employed to measure ion current density, Langmuir probes were used to measure the electron temperature and number density, and emissive probes were employed to measure the local plasma potential. In Figs. 5a and 5b radial profiles are shown of electron temperature at 10 and 50 mm from the thruster exit plane. The experimental uncertainty is reported to be $\pm 10\%$ (Ref. 16). For comparison the electron temperature of 3 eV assumed in the DSMC-PIC computations is also shown. Very close to the thruster, it is clear that there is significant variation in the electron temperature, because of the dynamics of the plasma generation inside the acceleration channel. However, at just 50 mm from the thruster, the electron temperature has decreased to about 3 eV and has a flat profile. This behavior is a result of the rapid expansion of the electrons away from the thruster and the neutralization process involving the electrons emitted by the cathode. Although it is expected that the electron temperature decreases at large distances from the thruster, it would appear that a value of 3 eV is a reasonable value for the simulations. The relative uniformity of electron temperature has been demonstrated experimentally for the SPT-100 Hall thruster by Myers and Manzella.²¹

The plasma potential profiles predicted by the simulation are compared with the experimental data of Ref. 16 in Figs. 6a and 6b again along radial lines located 10 and 50 mm from the thruster exit plane, respectively. All of the data are plotted relative to the cathode potential of 14 V. Close to the thruster, the simulation underpredicts the potential but does capture the shape quite well. At 50 mm from the thruster, the simulation and measured data are in excellent agreement.

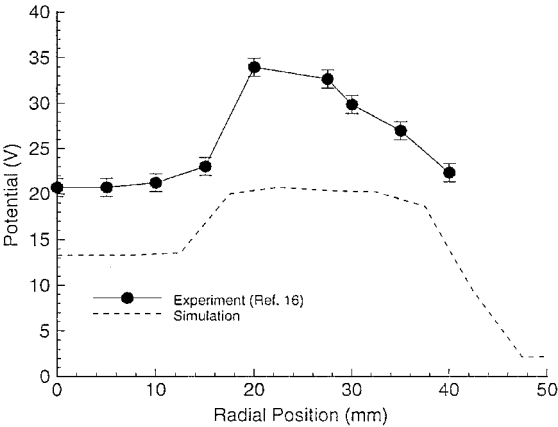


Fig. 6a Radial profile of plasma potential at 10 mm from the thruster exit plane.

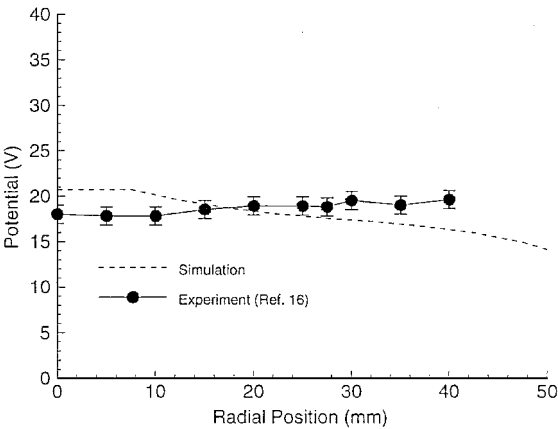


Fig. 6b Radial profile of plasma potential at 50 mm from the thruster exit plane.

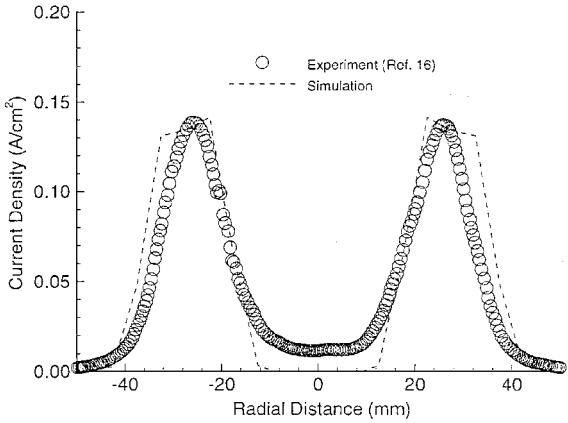


Fig. 7a Radial profile of ion charge density at 10 mm from the thruster exit plane.

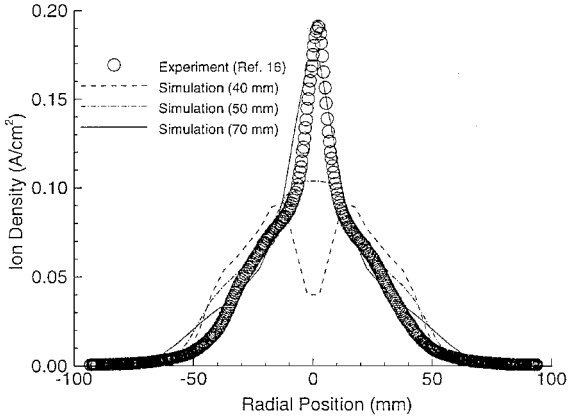


Fig. 7b Radial profile of ion charge density at 40 mm from the thruster exit plane.

In Figs. 7a and 7b the simulation and measured data for ion current density are compared at 10 and 40 mm from the thruster. In this case the simulation performs well close to the thruster but deteriorates at 40 mm. Also included in Fig. 7b are simulation profiles further from the thruster. The measured profile is produced in the simulation at a larger distance from the exit plane. This may indicate that despite the good agreement found in Fig. 7a, there are aspects of the simulation that do not accurately model the near-field plume behavior. In performing parametric studies the current density profile is very sensitive to the treatment of the radial velocity profile at the thruster exit.

Measurements of electron number density are compared with two sets of predictions at 10 and 50 mm in Figs. 8a and 8b, respectively. The predictions represent the total charge density obtained from the number densities of the Xe^+ and Xe^{++} ions. The reported error bars associated with this measurement are $\pm 50\%$ (Ref. 16). Therefore, most of the simulation data lies within this range although at the very lowest edge. The peak electron number density measured at both locations is more than double the total charge density assumed in the simulations at the thruster exit plane (see Table 1). There is no way to reconcile such a high electron number density with the measured device characteristics of current, specific impulse, and flow rate. Further direct evidence that the Langmuir probe technique leads to high electron number densities is provided in Ref. 17, where comparison is made with data acquired using microwave interferometry. At a distance of 25 cm from the thruster, the Langmuir probe electron number density was found to be a factor of six higher than the more reliable interferometry data.

Further comparisons between measured data and simulation results for electron number density in the far-field plume are shown in Figs. 9a–9c. The measured data were obtained by Gulczinski et al.¹⁷ using microwave interferometry. The uncertainty for these data is

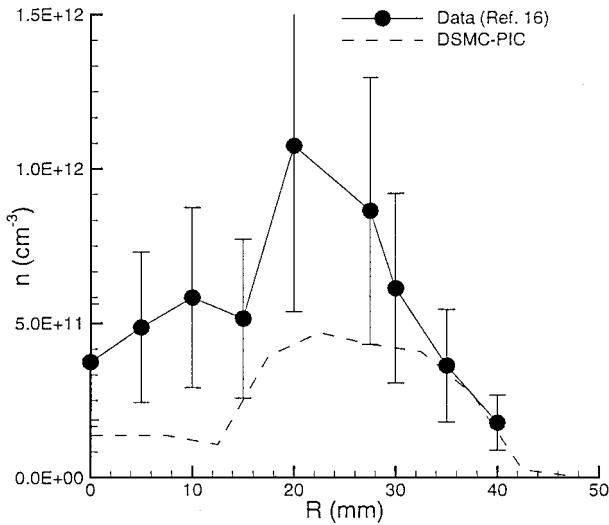


Fig. 8a Radial profile of electron number density at 10 mm from the thruster exit plane.

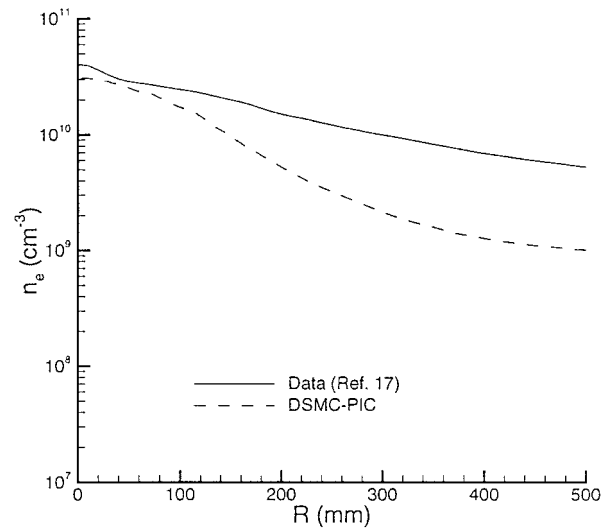


Fig. 9b Radial profile of electron number density at 50 cm from the thruster exit plane.

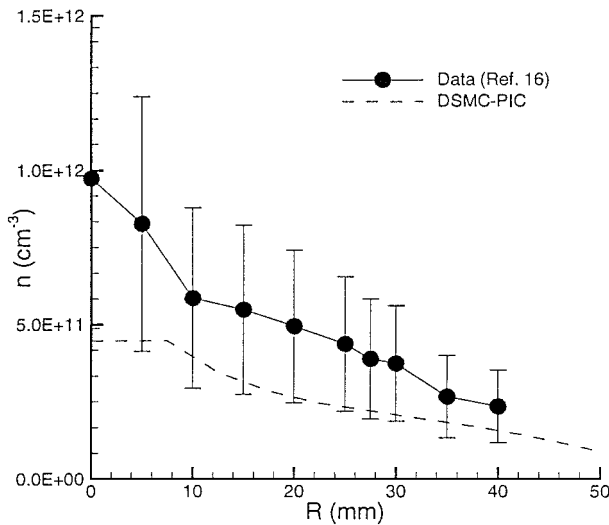


Fig. 8b Radial profile of electron number density at 50 mm from the thruster exit plane.

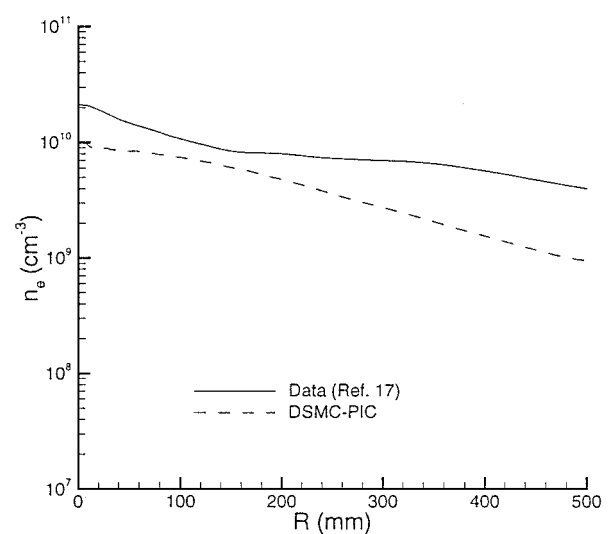


Fig. 9c Radial profile of electron number density at 100 cm from the thruster exit plane.

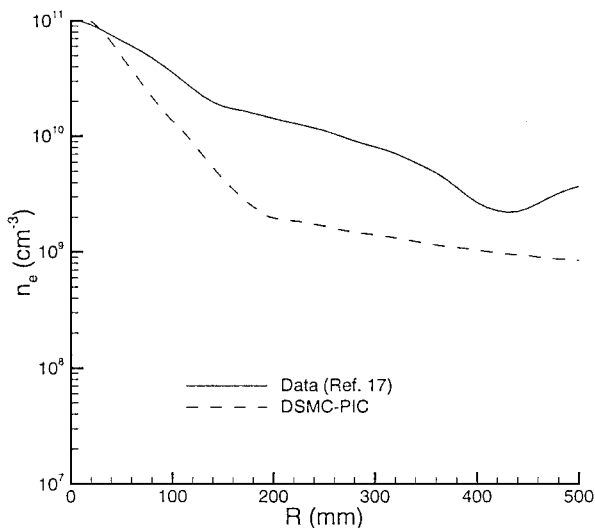


Fig. 9a Radial profile of electron number density at 25 cm from the thruster exit plane.

quoted as $\pm 10\%$. At a distance of 25 cm from the thruster, the simulation agrees with the measured data on the axis but underpredicts the density far from the axis. At further distances from the thruster, the agreement between the data sets on the axis deteriorates with the simulation predicting lower values in comparison to the measured data. At a distance of 100 cm from the thruster, the simulation result is a factor of two below the measurement. One interpretation of these comparisons is that the electric fields in the simulation are accelerating the ions too much in both the axial and radial directions. One possible explanation for such differences between the model and the measured data is the need to include partial confinement of electrons caused by the magnetic field of the thruster leaking into the near-field plume. It is also possible that the mechanism of source electron trapping proposed in Ref. 3 is important. Far-field measurements of plasma potential are required to help resolve this issue, and no such data presently exist.

A more detailed comparison between experiment and simulation is made in Fig. 10, which shows the ion energy distribution function at a distance of 50 cm from the point on the axis at the thruster exit plane for two different angles. The measured data were obtained for the SPT-100 Hall thruster using a molecular beam mass spectrometer (MBMS).¹⁸ Because of the similarities of the SPT and anode-layer devices, it is useful to compare the SPT measured data with the

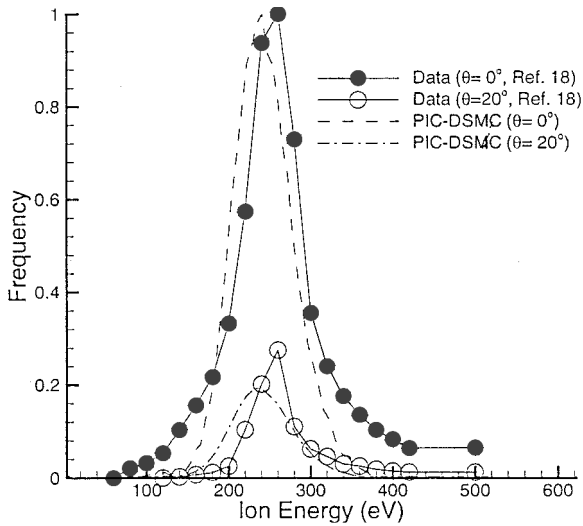


Fig. 10 MBMS ion energy distributions at a distance of 50 cm from the thruster.

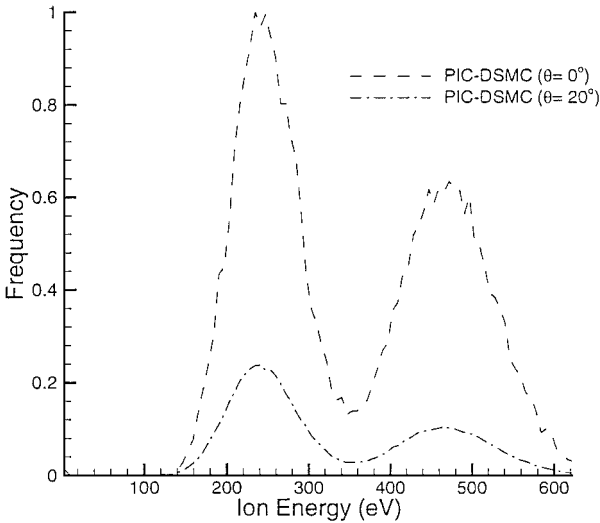


Fig. 11 True ion energy distributions at a distance of 50 cm from the thruster.

results predicted for the D55. As explained in Ref. 18, the energy detected by the MBMS is given by

$$E_{\text{ion}} = \frac{1}{2} m_i V_i^2 / q_i \quad (4)$$

where m_i is the ion mass, V_i is the ion velocity, and q_i is the ion charge. Thus, the instrument cannot directly detect the difference between single- and double-charged ions. The signal measured by the MBMS is an ion current, and so in the simulation the frequency is proportional to the velocity of each particle that crosses a fictional surface at the measurement location. Although all of the distributions in Fig. 10 have been normalized, the same normalization is employed in each data set for both of the angles. In general, the agreement between simulation and measurement is very good. The simulated distributions are shifted slightly to lower energy and are not as wide as the measured data. A small population of charge-exchange ions are predicted in the simulation at an ion energy of less than 5 eV. These populations are not visible in either the computed or measured data because the ion current contribution of the charge-exchange ions is very small. At energies above about 300 eV, there are significant differences between the measured and computed data. In particular, the experimental data contain an extended tail of high-energy ions that are not present in the computed data. If this high-energy tail does exist, it is perhaps created by plasma oscillations in the acceleration channel.

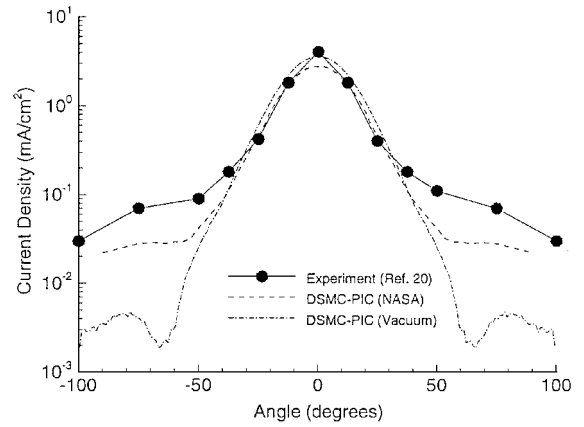


Fig. 12 Current density at a distance of 60 cm from the thruster.

In Fig. 11 the true ion energy distributions obtained from the simulation are shown at the same locations in the plume. In this case, unlike Eq. (4), the ion energy is not divided by the charge of the particle, and thus both the single- and double-charged populations are evident. Once again the frequency is computed as an ion current. Multiple ions play a significant role in determining the total ion current, and this is not evident from the data presented in Fig. 10. The development of a diagnostic that could resolve the behavior of each of the multiple ions would greatly benefit future modeling efforts.

Finally, the angular profile of current density at a distance of 60 cm from the thruster is considered in Fig. 12. The measurements were conducted in the NASA facility,²⁰ and the simulations use the second set of operating conditions given in Table 1. The level of agreement is quite good. The effect of the finite facility pressure is investigated through inclusion of a further simulation result computed for expansion into perfect vacuum. Clearly, facility-independent results are only obtained for angles up to about 45 deg.

Conclusions

A PIC-DSMC computer model of the D55 anode-layer Hall thruster plume has been developed that simulates ions and neutrals as particles and uses the Boltzmann relation to describe the electron number density. The effects of charge-exchange collisions and the finite pressure of experimental facilities were included in the model. Instead of assuming charge neutrality, the Poisson equation was solved to obtain the plasma potential. The use of the Boltzmann relation gave flow that was everywhere close to being charge neutral.

The comparisons of the simulation results with measured data generally indicated reasonable agreement. This was particularly true at distances beyond 10 mm from the thruster. Significantly, the good agreement was obtained using relatively simple assumptions about the properties of the beam emitted by the thruster. Thus, the present model is considered to be verified in the region close to the axis. Comparison of the simulation results with experimental measurements of electron number density in the plume far field showed significant differences. Specifically, the simulations underpredicted the density both on and off axis. It was speculated that this anomaly was caused by the simulated electric fields being too strong and therefore leading to overacceleration of the ions. Candidate physical mechanisms omitted from the present model that could account for such behavior include partial confinement of electrons by the magnetic field of the thruster leaking into the plume or by source electron trapping. Far-field plume measurements of plasma potential are required to resolve this issue.

Acknowledgment

Funding was provided by NASA Lewis Research Center under Grant NAG3-1451 with Eric Pencil as monitor. Many thanks to Matt Domonkos, Brad King, and Frank Gulczinski from the University of Michigan for sharing and explaining their data.

References

- ¹Samanta Roy, R. I., Hastings, D. E., and Gatsonis, N. A., "Ion-Thruster Plume Modeling for Backflow Contamination," *Journal of Spacecraft and Rockets*, Vol. 33, No. 4, 1996, pp. 524–534.
- ²VanGilder, D. B., Font, G. I., and Boyd, I. D., "Hybrid Monte Carlo Particle-in-Cell Simulation of an Ion Thruster Plume," *Journal of Propulsion and Power*, Vol. 15, No. 4, 1999, pp. 530–538.
- ³Katz, I., Davis, V. A., Wang, J., and Brinza, D., "Electric Potentials in the NSTAR Charge-Exchange Plume," International Electric Propulsion Conf., Paper 97-042, Aug. 1997.
- ⁴Birdsall, C. K., and Langdon, A. B., *Plasma Physics via Computer Simulation*, Adam Hilger Press, Bristol, England, UK, 1991.
- ⁵Bird, G. A., *Molecular Gas Dynamics and the Direct Simulation of Gas Flows*, Oxford Univ. Press, Oxford, England, UK, 1994.
- ⁶Fife, J. M., Martinez-Sanchez, M., and Szabo, J. J., "A Numerical Study of Low-Frequency Discharge Oscillations in Hall Thrusters," AIAA Paper 97-3052, July 1997.
- ⁷Boeuf, J. P., and Garrigues, L., "Low Frequency Oscillations in a Stationary Plasma Thruster," *Journal of Applied Physics*, Vol. 84, 1998, pp. 923–928.
- ⁸Oh, D., and Hastings, D. E., "Experimental Verification of a PIC-DSMC Model for Hall Thruster Plumes," AIAA Paper 96-3196, July 1996.
- ⁹Kim, S.-W., Foster, J. E., and Gallimore, A. D., "Very Near-Field Plume Study of a 1.35 kW SPT-100," AIAA Paper 96-2972, July 1996.
- ¹⁰Karabadzha, G. F., Semkin, A. V., Tverdoklebov, S. O., and Manzella, D. H., "Investigation of TAL Optical Emissions," International Electric Propulsion Conf., Paper 97-131, Aug. 1997.
- ¹¹Lago, V., de Graaf, M., and Dudeck, M., "Electron Energy Distribution Function in a Stationary Plasma Thruster Plume," AIAA Paper 97-3049, July 1997.
- ¹²Dalgarno, A., McDowell, M. R. C., and Williams, A., "The Mobilities of Ions in Unlike Gases," *Proceedings of the Royal Society of London*, Vol. 250, 1958, pp. 411–425.
- ¹³Sakabe, S., and Izawa, Y., "Simple Formula for the Cross Sections of Resonant Charge Transfer Between Atoms and Their Ions at Low Impact Velocity," *Physical Review A*, Vol. 45, No. 3, 1992, pp. 2086–2089.
- ¹⁴Boyd, I. D., "Conservative Species Weighting Scheme for the Direct Simulation Monte Carlo Method," *Journal of Thermophysics and Heat Transfer*, Vol. 10, No. 4, 1996, pp. 579–586.
- ¹⁵VanGilder, D. B., and Boyd, I. D., "Particle Simulations of the SPT-100 Plume," AIAA Paper 98-3797, July 1998.
- ¹⁶Domonkos, M. T., Marrese, C. M., Haas, J. M., and Gallimore, A. D., "Very Near-Field Plume Investigations of the D55," AIAA Paper 97-3062, July 1997.
- ¹⁷Gulczinski, F. S., Gallimore, A. D., Carlson, D. O., and Gilchrist, B. E., "Impact of Anode Layer Thruster Plumes on Satellite Communications," AIAA Paper 97-3067, July 1997.
- ¹⁸King, L. B., "Transport-Property and Mass Spectral Measurements in the Plasma Exhaust Plume of a Hall-Effect Space Propulsion System," Ph.D. Dissertation, Dept. of Aerospace Engineering, Univ. of Michigan, Ann Arbor, MI, May 1998.
- ¹⁹Semenkin, A., Kochergin, A., Garkusha, V., Chislov, G., Rusakov, A., Tverdoklebov, S., and Sota, C., "RHETT/EPDM Flight Anode Layer Thruster Development," IEPC, Paper 97-106, Aug. 1997.
- ²⁰Manzella, D. H., and Sankovic, J. M., "Hall Thruster Ion Beam Characterization," AIAA Paper 95-2927, July 1995.
- ²¹Myers, R. M., and Manzella, D. H., "Stationary Plasma Thruster Plume Characteristics," IEPC, Paper 93-096, Sept. 1993.